

Optimizing Connectivity: DVB-RCS2 Uplink to GEO Satellites via Optical Wireless Communication

Meryem Romaissa Djellouli^{1*}, Sid Ahmed Chouakri¹,
Abdelkrim Ghaz², and Taleb Ahmed Abdelmalik³

¹Telecommunications and Digital Signal Processing Laboratory, Djillali Liabes University, Sidi Bel Abbes, Algeria

²Communications Networks Architecture and Multimedia Laboratory, Djillali Liabes University, Sidi Bel Abbes, Algeria

³IEMN UMR CNRS 8520, Polytechnic University of Hauts, Valenciennes, France

ABSTRACT: This research focuses on the integration of an opto-satellite system based on Free Space Optical Communication (OWC) within DVB-RCS2 chains, implementing 16-QAM modulation techniques and Optical Time Division Wavelength Multiplexing (OTDM-WDM). A co-simulation framework combining the MATLAB and OptiSystem environments is adopted to evaluate the system's performance. Key performance indicators, such as Bit Error Rate (BER) and Q factor, are meticulously analyzed to quantify the effectiveness of the proposed approach. The results obtained demonstrate notable improvements in transmission reliability and signal quality, highlighting the potential of OWC to optimize DVB-RCS2 standards. This study significantly contributes to the development of innovative solutions in the field of satellite communications, paving the way for more efficient and resilient systems.

1. INTRODUCTION

Over the decades, the evolution of telecommunications networks has underscored the critical need for robust, international links. While technologies like coaxial cables, electromagnetic waves, and twisted pairs were initially used to improve data sharing, they could not keep up with growing data demands [1]. Today, OWC, especially outdoor free-space optics (FSO), is a proven method for connecting networks, often outperforming radio frequency (RF) communications, as shown in our studies [2–4]. Indeed, optical wireless communication offers several notable advantages over RF technologies, such as high data rates, high bandwidth, low latency, and optimized power consumption, thus meeting the growing requirements of next-generation networks, including 5G and 6G NTN (Non-Terrestrial Networks) [5, 6]. This technology offers high directivity, long-range operations, fast and easy deployment, low bit error rate, and enhanced security, as light waves do not penetrate through physical obstacles such as walls, reducing the risk of data interception [5]. These advantages, coupled with the fact that it is more resistant to harsh atmospheric conditions than RF methods, make it a promising solution. For example, rain attenuation is often less significant for FSO systems than radio systems. Using wavelengths such as 1550 nm reduces losses due to atmospheric absorption, improving transmission in light rain. Techniques, such as Intensive Modulation (IM), including modulation formats such as On-Off Keying (OOK), Non-Return-to-Zero (NRZ), and linear modulations with Direct Detection (DD), all combined with Direct Detection (DD), enhance the efficiency of optical trans-

mission. By combining FSO systems with radio links, continuous connectivity is ensured, creating an efficient hybrid solution [7–9]. OWC leverages the already available optical spectrum, reducing installation costs and minimizing environmental impact. Currently, most Internet access is provided via Ka- and Ku-band frequencies. However, new industrial applications demand much higher bandwidth capacities than those available through radio frequencies, which are limited to a few GHz. In contrast, optical frequencies, which are not subject to spectral regulation, offer a potential bandwidth around 10 THz, significantly increasing the capacity of communication systems [10]. Satellite communications, supported by geostationary (GEO) satellites, guarantee high-speed global coverage via the proposed optical approach, OWC. Satellites can be classified into three orbital categories: Low Earth Orbit (LEO), at an altitude of less than 2,000 km, Medium Earth Orbit (MEO) at around 20,000 km [11], and Geostationary Orbit (GEO) at 35,800 km, where satellites move in phase with the Earth's rotation [12]. Recent demonstrations have shown that data rates up to 1.72 Tbit/s are achievable via optical communications between a ground station and a geostationary satellite [10], as well as through inter-satellite links (ISL) using various modulations [13]. These results illustrate the potential of OWC to improve system performance. In addition, the application of OWC in direct links complying with DVB-S2 (Digital Video Broadcasting-Satellite 2) standards has also shown promising results [14, 15], prompting us to consider its use with the recently proposed satellite standards, DVB-RCS2 (Digital Video Broadcasting-Return Channel via Satellite 2). In short, the integration of OWC into satellite systems represents a major step forward in meeting today's connectivity challenges. At the intersection of optical communication and space appli-

* Corresponding author: Meryem Romaissa Djellouli (meryemromaissa1@gmail.com).

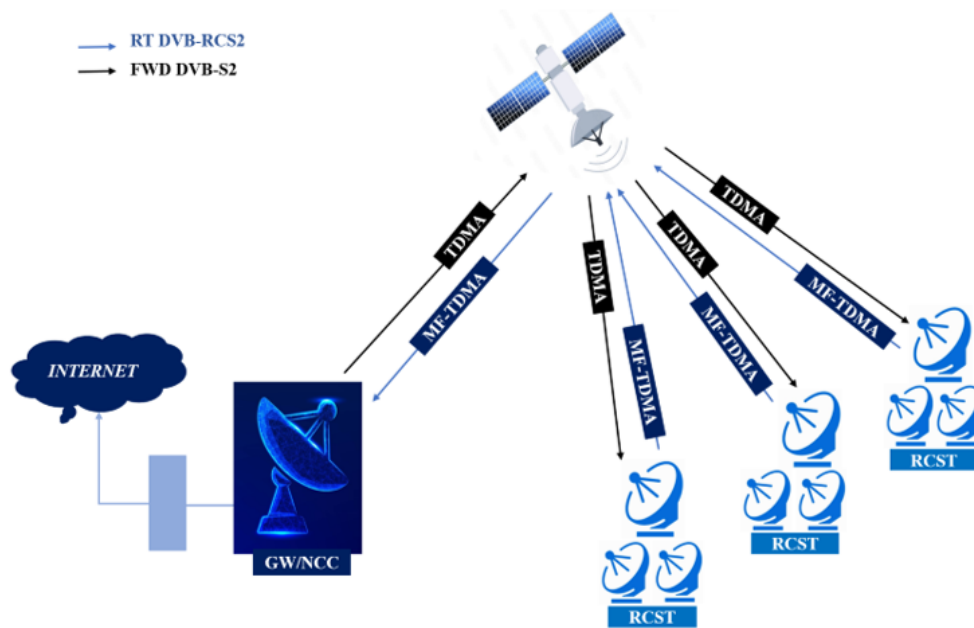


FIGURE 1. DVB-RCS2 system [20].



FIGURE 2. Burst waveform generation DVB-RCS2 [21].

cations, this article examines the application of Optical Wireless Communication (OWC) in the uplink channels of DVB-RCS2 systems using satellites in geostationary orbit, through a MATLAB-OptiSystem co-simulation.

2. SYSTEM STRUCTURE

2.1. Digital Video Broadcasting --- Return Channel via Satellite /2 (DVB-RCS/RCS2)

The DVB-RCS is a recent extension of the DVB broadcasting organization, specified in the ETSI EN 301.790 standard [16]. It establishes open international standards linked to direct systems like DVB-S and its enhancement, DVB-S2, facilitating internet access and data transport via satellite [17]. In 2012, the RCS standard advanced to the second generation, DVB-RCS2, incorporating data modeling and advanced physical equipment [18]. The architecture of DVB-RCS2 systems, illustrated in Fig. 1, utilizes DVB-S2 and DVB-RCS2 standards for channel access in both forward (from Gateway, GW, to Return Channel Satellite Terminal, RCST) and return directions. This structure includes multiple gateways (GWs) and a Network Control Center (NCC) for resource management. Interactive satellite terminals are connected to the external network via the GW/NCC gateway, using bidirectional MF-TDMA access mode in the Ka band [19].

An essential aspect of the DVB-RCS2 standard, illustrated in Fig. 2 [21], is its burst waveform structure, specifically designed to enhance communications in a context where spectral

resources are precious. It is specifically designed for seamless integration into satellite transmission systems that use multi-frequency time division multiple access (MF-TDMA). The wave structure includes essential elements such as energy distribution, the integration of cyclic redundancy checks (CRC) to detect errors, and the incorporation of unique words or pilot signals to ensure precise synchronization. Turbo coding is used for linear modulation to improve error efficiency, while convolutional coding is used for CPM (Continuous Phase Modulation). The burst waves of DVB-RCS2 present themselves as a solid and high-performing solution, perfect for reliable high-speed satellite communications [21].

Each DVB-RCS2 waveform, identified by a unique identifier, is classified according to technical parameters such as pulse length and payload, which influence transmission capacity. The mapping format, encoding rate, and post-intro length contribute to transmission efficiency and error correction. The contents of Table 1 in [21], under the selection of $ID = 11$, are used in our simulation to optimize these parameters, thereby ensuring performance in line with the protocol specifications.

2.2. Optical Wireless Communication (OWC)

Optical Wireless Communication (OWC), revitalized by LED technologies and Continuous Wave (CW) light sources, has proved effective in rapidly restoring high-speed connectivity. It is essential to consider the effects of optical signal propagation in the atmosphere, as environmental conditions can affect trans-

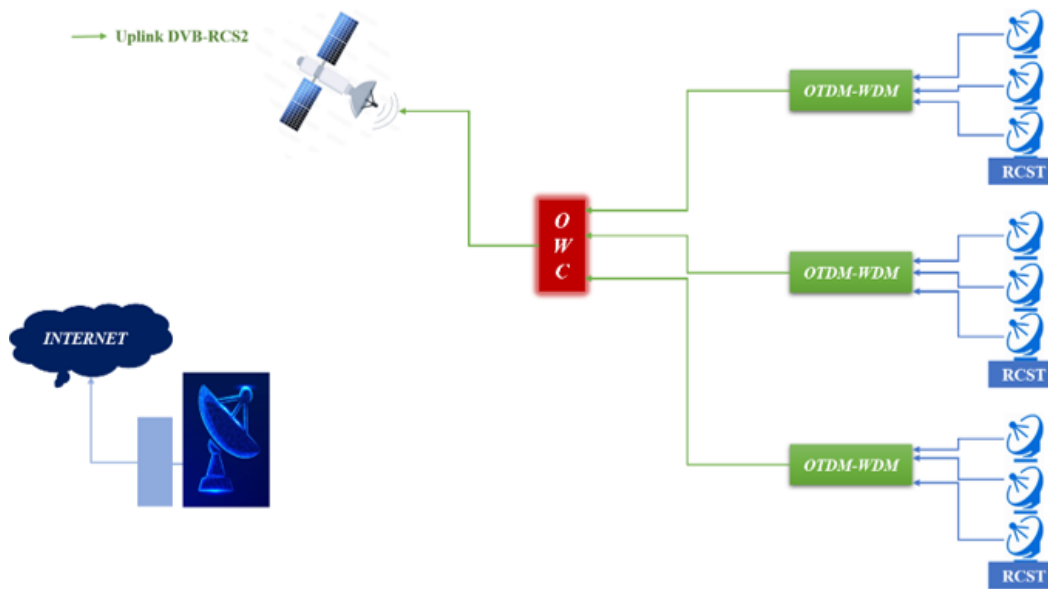


FIGURE 3. Uplink DVB-RCS2 OWC system.

mission quality. Attenuation caused by humidity reduces light intensity, while atmospheric turbulence causes fluctuations in the signal path, leading to distortion and loss of clarity. In addition, light scattering from particles in the air affects signal stability. Understanding these phenomena is essential for optimizing OWC systems and ensuring efficient and reliable data transmission [22].

2.3. OTDM-WDM

DVB-RCS2 streams are transmitted via MF-TDMA. Following our research [23–25], we have adapted our approach to integrate OWC into DVB-RCS2 systems by proposing OTDM-WDM as an equivalent hybrid solution. This model combines two optical techniques: OTDM (Optical Time Division Multiplexing), which divides time between users by allocating time slots for transmitting signals on a single wavelength, and WDM (Wavelength Division Multiplexing), which inserts several channels with different wavelengths into the same optical medium [26].

3. DESCRIPTION OF SYSTEM

3.1. Design of the DVB-RCS2 OWC System

This paper proposes the integration of optical wireless communication (OWC) into the DVB-RCS2 infrastructure. The proposed design, illustrated in Fig. 3, is based on DVB-RCS2-compliant channels using OWC optical media, including return channel satellite terminals (RCSTs) coordinated by a regenerative GEO satellite. Although Fig. 1 shows all possible combinations, our simulation focuses solely on connecting users to the satellite.

3.2. Implementation via Simulation

The structural diagram of the uplink (Uplink DVB-RCS2 OWC) describes the architecture for data transmission from several RCST subsystems to the geostationary satellite (GEO) at an altitude of 35,800 km via the OWC channel, using 16-QAM modulation and Turbo Codes (TC) integration. This is based on the information in Table 1 [21] with the selection of ID 11. Most existing studies have focused on inter-satellite links using only OptiSystem simulations. Although this research has explored various optical wireless communication (Is-OWC) techniques, it remains limited by challenges such as pointing errors and atmospheric turbulence [27–33]. With these limitations in mind, we proposed the idea of a co-simulation combining MATLAB and OptiSystem to better implement our system. This approach makes it possible to integrate and optimize the various components more effectively, offering a more efficient solution for high-speed data transmission over long distances between the RCSTs and the satellite.

TABLE 1. Parameters of DVB-RCS2 OWC link [38, 44].

Parameters	Values
Tx Aperture diameter (cm)	20.0
Rx Aperture diameter (cm)	25.0
Power transmission (dBm)	54.77
Gain transmission (dB)	112.2
Gain reception (dB)	114.1
Dark current (nA)	10
Responsivity of PIN (A/W)	1
Optical loss transmission (dB)	−3
Optical loss reception (dB)	−3
WDM frequency spacing (nm)	0.8

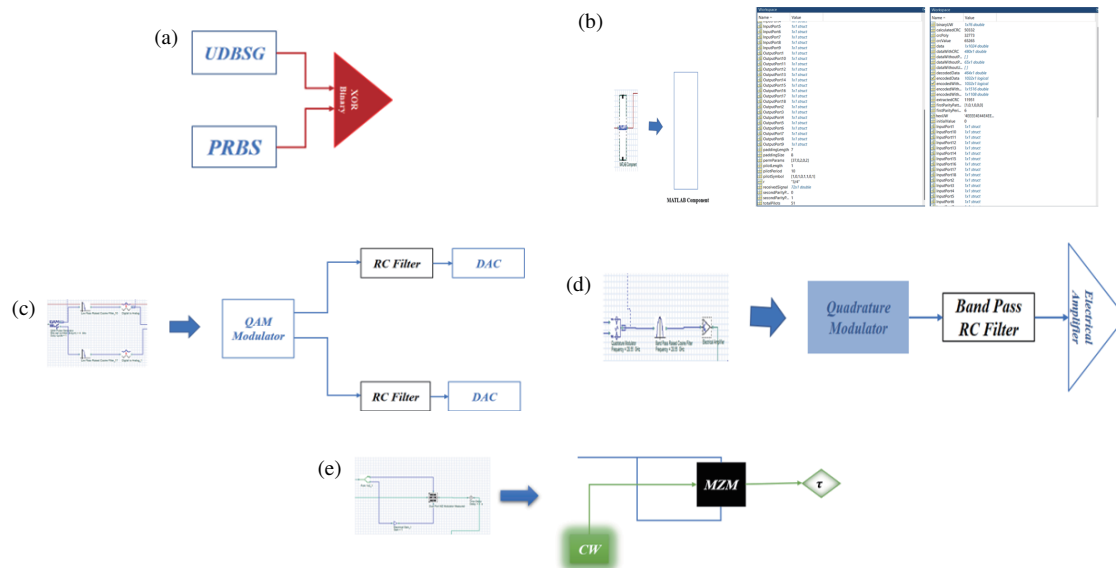


FIGURE 4. (a) Sequence processing; (b) Process configuration; (c) Modulation/Filtering/Conversion/ D/A Blocks; (d) ODU Process; (e) E/O Process.

3.2.1. At the RCST

The structure of satellite terminals (RCSTs) is divided into two primary components: Indoor Unit (IDU) and Outdoor Unit (ODU). The IDU encompasses baseband transmission functions and satellite modem tasks, facilitating connections with user terminals for access to the DVB-RCS2 network [34]. The ODU interfaces with the L-band IDU and comprises the antenna and RF electronics. DVB-RCS2 data transmission occurs as Intermediate Frequency (IF) signals, ranging from 0.95 to 1.45 GHz in the L-band, adhering to the standards established for all RCSTs [35]. Initially, the technical processing of the transmitting terminals, illustrated in Fig. 4(a), is discussed using functional diagrams. These diagrams incorporate a PRBS (Pseudo-Random Bit Sequence) to generate pseudorandom data, as well as a User Defined Bit Sequence Generator (UDBSG) to produce a specific sequence. Initially, the technical processing of the transmitting terminals, illustrated in Figure (a.4), is discussed using functional diagrams. These diagrams incorporate a PRBS (Pseudo-Random Bit Sequence) to generate pseudorandom data, as well as a User Defined Bit Sequence Generator (UDBSG) to produce a specific sequence. As shown in Table 1 and the conformity of the creation of the PDU (Protocol Data Unit) frame of the DVB-RCS2 standard [36], the creation of the PDU requires several parameters to be set. In this configuration, the PayloadLabel field is omitted, although it can be used to include additional information associated with the payload if required. The frame comprises two PPDUs (Payloadadapted PDU): the first takes up 85 bytes and the second 90 bytes, allowing the payload to be distributed efficiently while still meeting the format requirements. The PM (Payload header Map) field, which could also be included for additional functionality, is not used in this example. This structure ensures that the frame respects the 175-byte limit. Subsequently, a 9-byte preamble is included before the PDU frame to allow the receiver to synchronize the transmitted signal with

the receiver. This preamble ensures that the receiver can identify the start of the frame and prepare to understand the relevant information.

This frame is represented in binary form, saved as a file.txt, and then converted to a file.DAT, ready for integration into the OptiSystem software for optical analysis. Following the defined characteristics of the generators, a binary XOR operation is applied, combining the sequences from the UDBSG and the random data generator to ensure optimal energy dispersion in the signal.

Following the optimal dispersion of energy, the transmission process proceeds through several essential steps to ensure signal reliability, in accordance with the DVB-RCS2 transmission channel illustrated in Fig. 2 and the parameters described in Table 1 [21]. The data undergo a Cyclic Redundancy Check (CRC) to detect and correct any potential errors. Subsequently, Turbo coding is applied with a code rate of $\frac{3}{4}$ and permutation parameters $P = 37$, $Q_0 = 0$, $Q_1 = 2$, $Q_2 = 0$, $Q_3 = 2$, thereby enhancing the robustness of the signal by distributing errors across multiple symbols, alongside parity bits (First parity bit Y puncture = 20; 10001000100010000000, Second parity bit W puncture 1; 0) and the codeword $U_W = 4EEEE4E4E4EEEE4E4$. This method reduces the impact of interference and disturbance on signal quality. At the same time, specific pilots are inserted at regular intervals. With a pilot period of 10 symbols, a pilot block length of 1 symbol, and a total of 51 pilot symbols, this configuration ensures precise synchronization and reliable signal detection. In addition, a 9-byte post-amble is included after the payload and pilot, which marks the end of the frame and ensures that the receiver can identify the end of the transmission. This promotes signal stability during transmission. The configuration is described using MATLAB code, which is subsequently integrated into an existing MATLAB component within OptiSystem, through specific inputs and outputs for each user (for example: User 1:

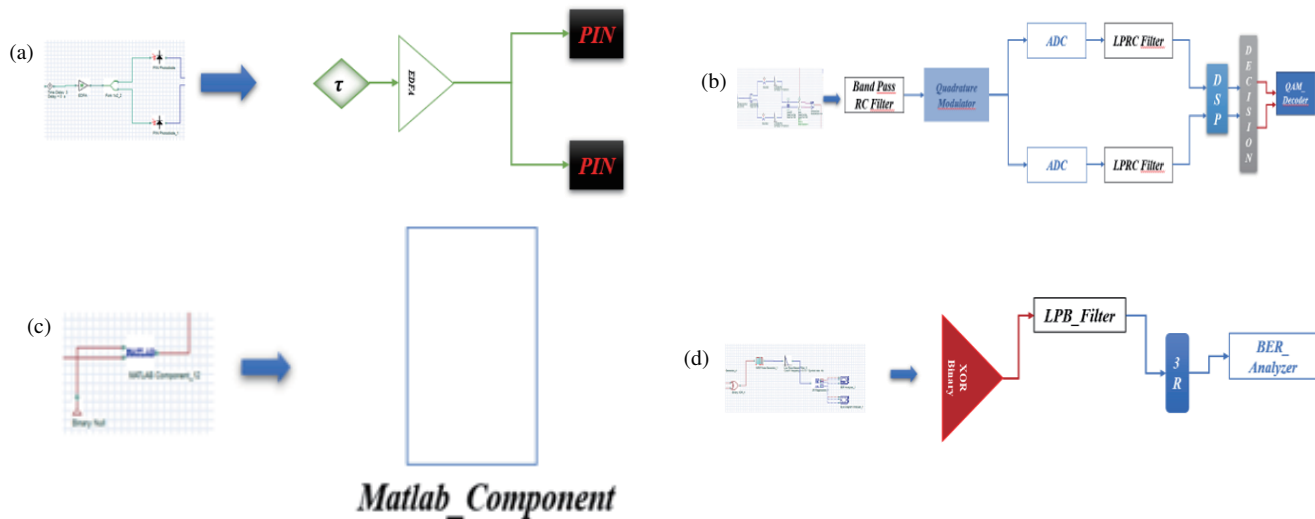


FIGURE 5. (a): O/E; (b): The LNB/DSP/decision/decoder; (c): MATLAB-component; (d): XOR/BER analyzer.

InputPort1; OutputPort1 for the transmission portion, and InputPort2; OutputPort2 for the reception portion under the GEO satellite). Fig. 4(b) illustrates the MATLAB workspace and the MATLAB component presented in OptiSystem. In Fig. 4(c), the symbols thus processed pass through the modulation process. Modulation is carried out using 16-QAM (Quadrature Amplitude Modulation), a technique that enables multiple bits per symbol to be transmitted by modifying both the amplitude and phase of the signal. This method offers increased spectral efficiency, enabling more data to be transmitted in the same frequency spectrum. Next, a Raised Cosine filter is applied to shape the signal and reduce inter-symbol interference. After this step, the symbols are routed through a digital-to-analog converter (DAC), with a 6-bit resolution determined by the DAC specifications [37], to perform digital-to-analog conversion and facilitate intermediate frequency (IF) transformation. The technical procedure, shown in Fig. 4(d), initiated within the ODU, is integrated into the BUC (Block Up-Converter). The latter incorporates a quadrature modulator, whose mission is to transpose DVB-RCS2 beams into RF signals, covering a frequency range between 29.5 and 30 GHz. This transposition is carried out using a local oscillator frequency set at 28.55 GHz, operating in the Ka-band [35]. Following this step, the signals are filtered to select the appropriate frequency band, then amplified before being directed to the next segment of the system.

As they pass through the system, the beams undergo an essential transition from RF to optical format, embodied in the electrical-to-optical (E/O) conversion process. This transformation is achieved through Mach-Zehnder modulators, which are strategically interfaced with optical laser sources operating in Continuous Wave (CW) mode. Subsequently, the optical signal is transmitted to the time-delay component, with a delay specified for each user by the formula $\tau_{\text{OTDM}} = \frac{T_{\text{OTDM}_b}}{N_{\text{OTDM}}}$, the delay required for each path is given by $\Delta\tau_{\text{OTDM}}(i) = i \times \frac{T_{\text{OTDM}_b}}{N_{\text{OTDM}}}$, where $i = 0, 1, 2, 3, \dots, N_{\text{OTDM}}-1$. In this method, the OTDM theorem can be applied within the user structure, where T_{OTDM_b} represents the bit duration, and N_{OTDM} is the number of users

in the OTDM system, as shown in Fig. 4(e), where $N_{\text{OTDM}} = 0, 1, 2, 3, \dots$. In this method, the OTDM theorem can be applied within the user structure, where T_{OTDM_b} represents the bit duration, and N_{OTDM} is the number of users in the OTDM system, as shown in Fig. 4(e).

3.2.2. At the GEO

The geostationary satellite (GEO) picks up the signals after a digital processing operation, playing a role similar to that of a telescope in receiver mode and thus constituting the signal's payload. As a result, signal intensity decreases, reaching power levels of the order of a few watts. To compensate for this loss, it is essential to pass them through devices capable of preamplifying the signal. In this context, low-noise optical amplifiers, known by the acronym LNOA (Low Noise Optical Amplifier), are essential, and in OptiSystem they are represented by EDFA (Erbium-Doped Fiber Amplifier) amplifiers [38]. Initially, by the OTDM-WDM inverse multiplexing principle, DVB-RCS2 beams are demultiplexed via WDM demultiplexers and OTDM power splitters, separating the individual channels and then assigned to the corresponding channels. These channels are then converted using optoelectronic (O/E: optical/electric) devices notably, (PIN, positive-Intrinsic-Negative) [38], shown in Fig. 5(a), to recreate the electrical signals from the light rays detected at the output of the OWC system. Fig. 5(b) illustrates the following process: after conversion via the PIN photodetectors, the LNB (Low Noise Block) transposes the signals to the intermediate frequency (IF) range. The LNB, consisting of a Band-Pass Raised Cosine Filter and a quadrature modulator, is primarily responsible for down-conversion (DC) and for routing the signals to the ADC (Analogue-to-Digital Converter), making it easier to convert the data for subsequent extraction. The signals are then processed by the Digital Signal Processor (DSP), which intervenes at several levels of processing. It applies digital filtering to reduce interference, ensures channel equalization to compensate distortions experienced during

propagation, and performs time and frequency synchronization to align the received signals correctly [39]. After these steps, 16-QAM demodulation is performed, followed by the decision block, which selects the most likely symbols from the demodulated signal. The 16-QAM decoder extracts the initial digital data, ready for systematic processing. Via MATLAB-OptiSystem co-simulation, the shared data is in Table 1 [21]. We have implemented a process for processing the signal received under the file created in MATLAB and integrated under the MATLAB-component of the OptiSystem, starting with the conversion of a single hexadecimal word into binary, thus enabling easier manipulation of the data. Pilot symbols are then removed from the received signal, ensuring that only relevant data is processed. The single word is removed from the data, followed by the removal of the parity bits. This step is crucial in preparing the data for decoding, ensuring that only essential information is retained. A data length check is then performed for Turbo decoding, which is applied to the prepared data using specific parameters to optimize signal robustness and spread errors over several symbols. Finally, the CRC is extracted and checked to ensure data integrity, and the decoded data is stored in the output, enabling it to be used in subsequent processing steps. Fig. 5(c) shows the component involved in the technical operation described in this section. The extracted symbols undergo a binary XOR operation using a specialized circuit, thus performing the inverse operation of the energy dispersion. They then pass through a Bessel low-pass filter (LPBF), whose aim is to eliminate high frequencies and reform the signal to facilitate analysis. At the end of this integrated process, the processed signals become visible through a display device, such as the BER viewer, allowing a complete evaluation of the transmission system's performance. Fig. 5(d) shows the final phase of processing.

3.3. Simulation Parameters

The proposed model was simulated with a power of 54.77 dBm at an optical wavelength of 1550 nm (nanometers) [40], the most commonly used in network infrastructures via optical wireless communication, an altitude of 35,800 km, and a throughput adapted to the specifications of our system. This data rate was determined using a bandwidth (BW) of 10 MHz [41, 42] and 16-QAM modulation combined with a turbo code rate of 3/4. With this configuration, we obtained a useful throughput of around 22 Mbps by calculating the symbol rate (R_s), which represents the modulation speed [43].

$$R_s = \frac{BW}{1 + \alpha} = \frac{10}{1 + 0.35} = 7.41 \text{ Ms/s} \quad (1)$$

The gross flow rate D_b is then determined using the following formula:

$$D_b = \log_2(M) \times R_s = \log_2(16) \times 7.41 \approx 29.64 \text{ Mbps} \quad (2)$$

Take into account the useful flow D_u as follows:

$$D_u = D_b \times \frac{3}{4} = 22.23 \text{ Mbps} \quad (3)$$

Table 1 shows the parameters of the DVB-RCS2 OWC Link.

3.4. Performances Evaluation

-The Q factor:

This is a quality measure that allows the signal to be quantified and evaluated without having to directly count the errors given by:

$$Q = \frac{V_1 - V_0}{\sigma_1 + \sigma_0} \quad (4)$$

V_0 and V_1 are the average voltages of levels 1 and 0, and σ_0 and σ_1 represent the variances of the probabilities of the powers of levels 1 and 0. In optical communication, the acceptable value for this factor is 6 dB [45].

-Bit error rate (BER):

This is a parameter which indicates the ratio of transmitted bits to erroneous bits. A system is generally considered to be of good quality in optical telecoms if its BER is less than 10^{-9} . The bit error rate and Q factor are linked by the following equation [45]:

$$\text{BER} = \frac{1}{2} \text{erfc} \left(\frac{Q}{\sqrt{2}} \right) \quad (5)$$

-Eye diagram

This is a qualitative factor that gives an idea of noise amplitude, interference, and time jitter. It represents all the symbols of the transmitted signal superimposed on each other [45].

-Packet Error rate (PER)

The packet error rate is a functional indicator of the quality of service that can be evaluated. It is defined as the proportion of data packets received by the destination over a wireless link that contains one or more burst errors. The packet error rate is calculated using the following formula [46].

$$\text{PER} = 1 - (1 - \text{BER})^L \quad (6)$$

with L being the number of bits in the packet.

- Received power

The link estimate for an uplink channel therefore adds back to the power received at the receiver end, which corresponds to the equivalent isotropically radiated power (EIRP), segmented by the losses on the receiver paths. This is expressed by the Friis equation below [47]:

$$P_R(\text{GEO}) = \frac{P_E(\text{ES}) \cdot G_e(\text{ES}) \cdot G_r(\text{GEO})}{\left(\frac{4\pi d}{\lambda}\right)^2} \quad (7)$$

With

$$L_{FSO} = \left(\frac{4\pi d}{\lambda}\right)^2 \quad (8)$$

$P_{E(\text{Earth_station})}$: the power supplied by the transmitting antenna of the RCST system (in Watt), $G_{E(\text{Earth_station})}$: the gain in the transmitting mode of the RCSTs, $G_{R(\text{GEO})}$: the gain of a satellite receiving antenna, and L_{FSO} : the attenuation due to propagation in free space.

$$P_R(\text{GEO}) = P_{E(\text{ES})} + G_{E(\text{ES})} + G_{R(\text{GEO})} - (L_{FSO} + L_{Tx} + L_{Rx} + L_{ATM}) \quad (9)$$

$P_{E(\text{ES})}$ in dBm, $G_{E(\text{ES})}$, $G_{R(\text{GEO})}$, L_{ATM} , L_{FSO} , and L_{Tx} , L_{Rx} are in dB.

TABLE 2. Performance of DVB-RCS2 OWC.

User	BER	Q Factor (dB)
1	5.3×10^{-22}	9.57
2	3.0×10^{-22}	9.63
3	2.3×10^{-22}	9.66
4	4.3×10^{-22}	9.59
5	3.9×10^{-22}	9.60
6	1.6×10^{-22}	9.70
7	3.1×10^{-22}	9.63
8	1.2×10^{-22}	9.72
9	6.1×10^{-22}	9.56

TABLE 3. DVB-RCS2 without OWC and other studies.

User	Without OWC		Other Studies	
	BER	Q (dB)	BER	Q (dB)
1	1.5×10^{-1}	0.2	8.9×10^{-2}	1.3
2	1.3×10^{-1}	1.1	7.9×10^{-2}	1.4
3	1.9×10^{-1}	-1.1	4.6×10^{-2}	1.6
4	1.7×10^{-1}	-0.4	9.2×10^{-9}	5.6
5	1.4×10^{-1}	0.9	1.3×10^{-4}	3.6
6	1.3×10^{-1}	1.0	1.7×10^{-4}	4.6
7	1.4×10^{-1}	0.7	1.9×10^{-4}	3.5
8	1.7×10^{-1}	-0.3	1	0
9	2.3×10^{-1}	-2.5	9.5×10^{-4}	3.1

TABLE 4. Received power values.

Power	Calculated	Simulated
$P_{r(GEO)}$	-12.33 dBm (58.4×10^{-6} W)	-13.58 dBm (43.82×10^{-6} W)

With L_{ATM} : the atmospheric losses, L_{Tx} : transmission losses between the transmitter and the transmitting antenna, and L_{Rx} : reception losses between the receiving antenna and the receiver [47].

4. RESULTS AND DISCUSSION

4.1. Results

Based on our analysis of DVB-RCS2 with OWC, the following Tables 2 and 4 present the results for three parameters compared to the theoretical equations mentioned above (4, 5, and 10), thus, Table 3 also includes the results of the comparison between DVB-RCS2 using RF transmission without OWC and those of the results of other studies on similar technologies.

4.2. Discussion

The limited performance of radio frequency (RF) transmission systems prompted us to explore more robust alternatives, leading to the creation of an optical bridge based on DVB-RCS2 technology. This initiative is based on integrating MATLAB code into OptiSystem and the characteristics defined in Table 1. The results obtained, detailed in Tables 2 and 4, together with the analysis of the eye diagrams (Fig. 6), demonstrate the effectiveness of this approach. The key performance criteria, namely the bit error rate (BER) and quality factor (Q factor), achieved promising values, with a BER of around 10^{-9} and a Q factor greater than 6 dB. These results reflect excellent signal integrity, guaranteeing reliable, high-quality transmission. Furthermore, the simulated power values were very close to the expected theoretical ones, and the differences observed are mainly due to the inherent limitations of the software simulations and the absence of physical equipment (Fig. 7). The implementation of DVB-RCS2 without OWC shows limited results compared to our results. Furthermore, a comparison

with similar technologies using OWC has been carried out (Table 3) [48, 49]. Concerning other studies [50] and by the choice of ID = 11 in Table 1 [21], we obtained a packet error rate (PER) close to zero. Our approach stands out for its high competitiveness in information transmission, demonstrated by the quality of the signals transmitted and the performance robustness under simulated conditions. This competitiveness is based not only on the integration of optical communications but also on the optimal exploitation of the advantages of DVB-RCS2. Given the constraints of RF systems, which are characterized by limited bandwidth, increased interference, and greater sensitivity to environmental conditions, OWC is a strategic alternative to our proposed system. The integration of OWC into our DVB-RCS2 network has resulted in even more robust performance, thanks in particular to using 16-QAM constellations in DVB-RCS2 uplinks. Recognized for its ability to carry large amounts of data compared with other modulation formats, 16-QAM has made it possible to increase spectral density while maintaining acceptable error levels. The oscillograms of the eye obtained show ideal characteristics for transmission: sufficient width to guarantee precise synchronization of successive samples and adequate height to reflect an optimum signal-to-noise ratio. In conclusion, this interpretation demonstrates that the integration of OWC technology with DVB-RCS2 provides a highly competitive solution for information transmission, particularly in environments where bandwidth and signal quality are priorities. By leveraging the advantages of optical communications and advanced modulation techniques, our system significantly enhances telecommunications network performance while meeting the increasing demands for high-speed data transmission. However, our simulation is currently limited to a maximum of 9 users. This limitation warrants further study to enable a greater number of users while maintaining high throughput, presenting an interesting avenue for future research.

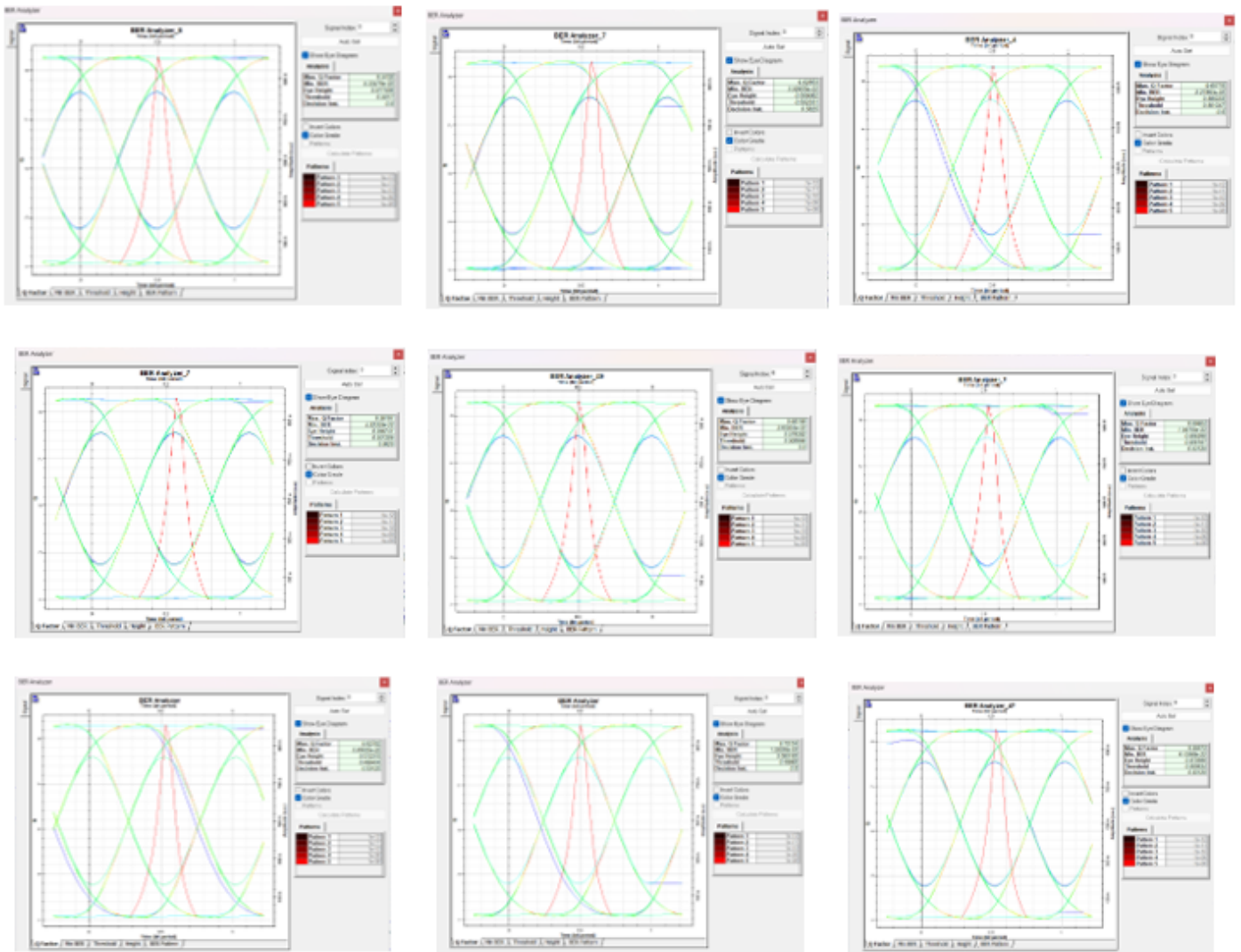


FIGURE 6. Eye diagrams of DVB-RCS2 OWC.

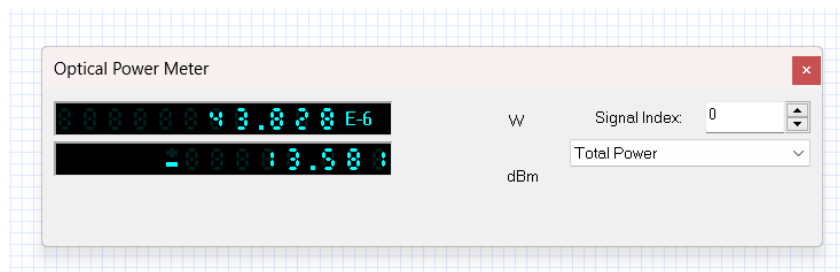


FIGURE 7. Power measurement in OptiSystem.

5. CONCLUSION AND PERSPECTIVE

As part of this practical analysis, the structural integration of the DVB-RCS2 system reveals significant interconnection via the OWC medium, with a substantial impact on link performance. This is based on an in-depth analysis of the estimated values for the three crucial indicators, carefully documented in the results tables and graphically illustrated in the eye diagrams presented. When we apply the optical laws to the space sector, the eval-

uation of the powers received at the receiving infrastructures proves to be in perfect correlation with the values of the theoretical proofs calculated. It is essential to emphasize that bit error rates (BERs) of less than 10^{-9} , and quality factors (Q) greater than 6 enhance the reliability and efficiency of the link. An in-depth analysis of the explanatory and comparative expressions allows us to state that the results obtained far exceed initial expectations, testifying to a very high level of satisfaction with

the performance of opto-spatial interconnection within DVB-RCS2 networks. This success is all the more significant given the ever-growing need for space communications. These encouraging results open up new prospects for considerably optimising the links of the entire RCST system, whether directly to the gateway (GW) or via relays between satellites, using optical wireless communication, while strengthening integration with our DVB-RCS2 system.

ACKNOWLEDGEMENT

This work was supported by the Directorate General for Scientific Research and Technological Development (DGRSDT).

REFERENCES

- [1] Bouchet, O., *Wireless Optical Communications*, John Wiley & Sons, 2013.
- [2] Garg, D. and A. Nain, "Next generation optical wireless communication: A comprehensive review," *Journal of Optical Communications*, Vol. 44, No. s1, s1535–s1550, 2023.
- [3] Djellouli, M. R., S. A. Chouakri, and A. Ghaz, "OWC Inter Satellite link throughput improvement based on WDM architecture," in *2022 2nd International Conference on Advanced Electrical Engineering (ICAEE)*, 1–6, Constantine, Algeria, Oct. 2022.
- [4] Djellouli, M. R., S. A. Chouakri, and A. Ghaz, "Inter-satellite simulation with custom modulation: Enabling DVB-RCS2 integration with optical communication networks," in *3rd Edition of the International Conference on Materials Science and Engineering and their Impact on the Environment (ICMSE'2024)*, Sidi Bel Abbès, Algeria, May 2024.
- [5] Jahid, A., M. H. Alsharif, and T. J. Hall, "A contemporary survey on free space optical communication: Potentials, technical challenges, recent advances and research direction," *Journal of Network and Computer Applications*, Vol. 200, 103311, 2022.
- [6] Elamassie, M. and M. Uysal, "Free space optical communication: An enabling backhaul technology for 6G non-terrestrial networks," *Photonics*, Vol. 10, No. 11, 1210, 2023.
- [7] Latal, J., J. Vitasek, L. Hajek, A. Vanderka, R. Martinek, and V. Vasinek, "Influence of simulated atmospheric effect combined with modulation formats on FSO systems," *Optical Switching and Networking*, Vol. 33, 184–193, 2019.
- [8] Naghshvarianjahromi, M., S. Kumar, and M. J. Deen, "Free space ground to satellite optical communications using Kramers-Kronig transceiver in the presence of atmospheric turbulence," *Sensors*, Vol. 22, No. 9, 3435, 2022.
- [9] Latal, J., J. Vitasek, M. Bojko, J. Skrinsky, T. Stratil, Z. Wilcek, and J. Kolar, "Simulation and measurement of atmospheric effect on optical beam," in *2018 20th International Conference on Transparent Optical Networks (ICTON)*, 1–7, Bucharest, Romania, 2018.
- [10] Poliak, J., R. M. Calvo, and F. Rein, "Demonstration of 1.72 Tbit/s optical data transmission under worst-case turbulence conditions for ground-to-geostationary satellite communications," *IEEE Communications Letters*, Vol. 22, No. 9, 1818–1821, 2018.
- [11] Jia, Z., C. Dong, K. Guo, and Q. Wu, "The potential of LEO satellites in 6G space-air-ground enabled access networks," *ArXiv Preprint ArXiv:2307.00234*, 2023.
- [12] Giordani, M. and M. Zorzi, "Non-terrestrial networks in the 6G era: Challenges and opportunities," *IEEE Network*, Vol. 35, No. 2, 244–251, 2020.
- [13] Abdulwahid, M. M. and S. Kurnaz, "The channel WDM system incorporates of Optical Wireless Communication (OWC) hybrid MDM-PDM for higher capacity (LEO-GEO) inter satellite link," *Optik*, Vol. 273, 170449, 2023.
- [14] Ahmad, I., K. D. Nguyen, N. Letzepis, and G. Lechner, "On the next-generation high throughput satellite systems with optical feeder links," *IEEE Systems Journal*, Vol. 15, No. 2, 2000–2011, 2020.
- [15] Gayrard, J.-D., A. Maho, and M. Sotom, "Free-space optical communication technologies will enable next generation of ultra high throughput satellite," in *International Conference on Space Optics — ICSO 2021*, Vol. 11852, 2416–2424, 2021.
- [16] Stette, G., "The DVB RCS system advancing to new applications," in *24th AIAA International Communications Satellite Systems Conference (ICSSC)*, 5472, San Diego, CA, USA, Jun. 2006.
- [17] Vrščeká, M. and J. Kunický, "Satellite signal DVB-S2," in *2021 International Conference on Military Technologies (ICMT)*, 1–6, Brno, Czech Republic, Jun. 2021.
- [18] Skinnemoen, H., C. Rigal, A. Yun, L. Erup, N. Alagha, and A. Ginesi, "DVB-RCS2 overview," *International Journal of Satellite Communications and Networking*, Vol. 31, No. 5, 201–217, 2013.
- [19] Munari, A., G. Acar, C. Kissling, M. Berioli, and H. P. Lexow, "Multiple access in DVB-RCS2 user uplinks," *International Journal of Satellite Communications and Networking*, Vol. 32, No. 5, 359–376, 2014.
- [20] Marchese, M. and M. Mongelli, "Adaptive call admission and bandwidth control in DVB-RCS systems," *Journal of Communications and Networks*, Vol. 12, No. 6, 568–576, 2010.
- [21] Digital Video Broadcasting (DVB), "Second generation DVB interactive satellite system (RCS2); Part 2: Lower layers for satellite specification standard," Mar. 2010.
- [22] Chowdhury, M. Z., M. T. Hossain, A. Islam, and Y. M. Jang, "A comparative survey of optical wireless technologies: Architectures and applications," *IEEE Access*, Vol. 6, 9819–9840, 2018.
- [23] Djellouli, M. R., S. A. Chouakri, and A. Ghaz, "Towards establishing the correspondence of the DVB-RCS2 radio-frequency MF-TDMA with the optical OTDM/WDM," in *National Conference on Telecommunications and Its Applications (CNTA'22)*, Ain Témouchent, Algeria, Dec. 2022.
- [24] Djellouli, M. R., S. A. Chouakri, and A. Ghaz, "Implementation of MF-TDMA OTDM-WDM mapping for the DVB-RCS2 system: Functional approach," in *Proc. 1st Int. Conf. Advances in Electronics, Control and Computer Technologies*, Mascara, Algeria, Oct. 2023.
- [25] Djellouli, M. R., S. A. Chouakri, and A. Ghaz, "Exploring the equivalence of MF-TDMA and OTDM-WDM: A comparative study and prospects for integration in DVB-RCS2 networks," in *Proc. International Conference on Advances in Electrical and Communication Technologies (ICAECOT'24)*, Sétif, Algeria, Oct. 2024.
- [26] Mellia, M., E. Leonardi, M. Feletig, R. Gaudino, and F. Neri, "Exploiting OTDM technology in WDM networks," in *Proceedings Twenty-First Annual Joint Conference of the IEEE Computer and Communications Societies*, Vol. 3, 1822–1831, New York, NY, USA, Jun. 2002.
- [27] Chaudhary, S., A. Sharma, and N. Chaudhary, "6 × 20 Gbps hybrid WDM-PI inter-satellite system under the influence of transmitting pointing errors," *Journal of Optical Communications*, Vol. 37, No. 4, 375–379, 2016.
- [28] Chaudhary, S., X. Tang, A. Sharma, B. Lin, X. Wei, and A. Parmar, "A cost-effective 100 Gbps SAC-OCDMA-PDM based

- inter-satellite communication link,” *Optical and Quantum Electronics*, Vol. 51, 1–10, 2019.
- [29] Sharma, A., A. Parmar, P. Sood, V. Dhasratan, and C. Guleria, “Performance analysis of free space optics and inter-satellite communicating system using multiplexing techniques — A review,” *Journal of Optical Communications*, Vol. 42, No. 3, 465–470, 2021.
- [30] Chaudhary, S., A. Sharma, and V. Singh, “Optimization of high speed and long haul inter-satellite communication link by incorporating differential phase shift key and orthogonal frequency division multiplexing scheme,” *Optik*, Vol. 176, 185–190, 2019.
- [31] Sharma, A., J. Malhotra, S. Chaudhary, and V. Thappa, “Analysis of 2×10 Gbps MDM enabled inter satellite optical wireless communication under the impact of pointing errors,” *Optik*, Vol. 227, 165250, 2021.
- [32] Chaudhary, S., R. Kapoor, and A. Sharma, “Empirical evaluation of 4 QAM and 4 PSK in OFDM-based inter-satellite communication system,” *Journal of Optical Communications*, Vol. 40, No. 2, 143–147, 2019.
- [33] Chaudhary, S., L. Wuttisittikulij, J. Nebhen, A. Sharma, D. Z. Rodriguez, and S. Kumar, “Terabyte capacity-enabled (10 x 400 Gbps) Is-OWC system for long-haul communication by incorporating dual polarization quadrature phase shift key and mode division multiplexing scheme,” *Plos One*, Vol. 17, No. 3, e0265044, 2022.
- [34] Gheorghie, C.-G., “Improvements of DVB-RCS2 to DVB-RCS,” *Telecomunicații*, Vol. LVIII, No. 1, 31–37, 2015.
- [35] ETSI, “Digital video broadcasting (DVB); second generation dvb interactive satellite system (DVB-RCS2); part 4: Guidelines for implementation and use of en 301 545-2,” Apr. 2014.
- [36] ETSI, “Satellite earth stations and systems (SES); return link encapsulation (RLE) protocol,” Jun. 2023.
- [37] Roy, B., S. Poulencard, S. Dimitrov, R. Barrios, D. Giggenbach, A. L. Kerneec, and M. Sotom, “Optical feeder links for high throughput satellites,” in *2015 IEEE International Conference on Space Optical Systems and Applications (ICSOS)*, 1–6, New Orleans, LA, USA, Oct. 2015.
- [38] Dimitrov, S., R. Barrios, B. Matuz, G. Liva, R. Mata-Calvo, and D. Giggenbach, “Digital modulation and coding for satellite optical feeder links with pre-distortion adaptive optics,” *International Journal of Satellite Communications and Networking*, Vol. 34, No. 5, 625–644, 2016.
- [39] Romanato, R., G. D’Angelo, G. Gallinaro, H. Brandt, and H. Bischl, “Study and implementation of a next generation regenerative on board processor emulator,” in *2016 8th Advanced Satellite Multimedia Systems Conference and the 14th Signal Processing for Space Communications Workshop (ASMS/SPSC)*, 1–7, Palma de Mallorca, Spain, Sep. 2016.
- [40] Vidal, O., B. Roy, S. Dimitrov, R. Barrios, D. Giggenbach, and A. L. Kerneec, “Next generation high throughput satellite system based on optical feeder links,” in *Proceedings of the Ka and Broadband Communications, Navigation and Earth Observation Conference*, Bologna, Italy, Oct. 2015.
- [41] Duverdier, A. and M. Bousquet, “High throughput satellites: Issues in comparing capacities,” in *2022 27th Asia Pacific Conference on Communications (APCC)*, 187–192, Jeju Island, Korea, Oct. 2022.
- [42] Tropea, M., P. Fazio, F. D. Rango, and A. F. Santamaria, “Novel MF-TDMA/SCPC switching algorithm for DVB-RCS/RCS2 return link in railway scenario,” *IEEE Transactions on Aerospace and Electronic Systems*, Vol. 52, No. 1, 275–287, 2016.
- [43] NERA, *Digital Video Broadcasting-Return Channel via Satellite DVB-RCS (Background Book)*, 1st ed., Nov. 2002.
- [44] Roy, B., S. Poulencard, S. Dimitrov, R. Barrios, D. Giggenbach, A. L. Kerneec, and M. Sotom, “Optical feeder links for high throughput satellites,” in *2015 IEEE International Conference on Space Optical Systems and Applications (ICSOS)*, 1–6, New Orleans, LA, USA, Oct. 2015.
- [45] Gay, M., “Theoretical and experimental study of the impact of 2R regeneration in a high-speed optical transmission system,” Ph.D. dissertation, Institut National des Sciences Appliquées de Rennes, France, 2006.
- [46] Pundir, M. and J. K. Sandhu, “A systematic review of quality of service in wireless sensor networks using machine learning: Recent trend and future vision,” *Journal of Network and Computer Applications*, Vol. 188, 103084, 2021.
- [47] Kassouri, M. and A. S. Ali, “The impact of meteorological phenomena on a satellite link: The case of a DVB-S link,” 2013.
- [48] Kaur, S. and A. Seehra, “Comparison of BER and Q-factor in an Is-OWC system using WDM with different modulation techniques,” in *2019 International Conference on Communication and Electronics Systems (ICCES)*, 448–453, Coimbatore, India, Jul. 2019.
- [49] Hasan, H. J., “Use the opti system program to determine the best suitable wavelength for sending data over long distances,” *IAR Journal of Engineering and Technology*, Vol. 4, No. 2, Jul. 2023.
- [50] Fenech, H., S. Amos, A. Tomatis, and V. Soumpholphakdy, “High throughput satellite systems: An analytical approach,” *IEEE Transactions on Aerospace and Electronic Systems*, Vol. 51, No. 1, 192–202, 2015.